Abortive Initiation and Productive Initiation by RNA Polymerase Involve DNA Scrunching

Andrey Revyakin, *et al.*

Science **314**, 1139 (2006);
DOI: 10.1126/science.1131398

Science (print ISSN 0036-8075; online ISSN 1095-9203) is published weekly, except the last week in December, by the American Association for the Advancement of Science, 1200 New York Avenue NW, Washington, DC 20005.

between the twin daughter cells (Fig. 4, D, F, and H, and figs. S14, C and D, and S15B), corresponding to a positional information distance of up to six cells (or 20 μm) (Fig. 4A). Distribution of nonphosphorylated Mad was not affected (fig. S13F). Thus, Sara endosomes store signaling molecules (receptors and/or transcription factors) and are partitioned into the twin daughter cells by association with the central spindle. Sara itself is required for central spindle targeting of the receptor cargo and ensures the maintenance of the levels of pMad within the gradient across mitosis.

The differences in pMad levels between twin sibling cells decrease with time after mitosis in Sara mutants, leading to an overall normal pMad gradient with normal amplitude and range in interphase cells (fig. S10). Consistently, wings of *sara*^{12} escapers did not exhibit large-scale Dpp-related patterning phenotypes (Fig. 4, L to Q). This result implies the existence of mechanisms that smooth the uneven signaling levels in Sara mutants after mitosis. These mechanisms may include the elimination of cells causing discontinuities in the pMad gradient by *brinker*-mediated apoptosis (*17*). Correspondingly, elevated apoptosis levels were observed both in Sara mutant wings (Fig. 4I and fig. S16, B, C, and E) and in Sara mutant clones relative to the surrounding tissue (fig. S16, A and D). Cells entering apoptosis, as monitored by the expression of head involution defective (Hid), exhibited elevated pMad levels in comparison with their neighbors (fig. S16F), which is consistent with previous observations (*18*, *19*). In contrast, daughter cells with inappropriately low signaling levels after mitosis appeared to recover in interphase, implying that, in the larval disk, there is time for de novo signaling by the extracellular gradient of Dpp before cells are committed to a specific fate.

Uneven signaling levels after mitosis should become fixed if differentiation occurred right after division. In the pupal wing, Dpp signaling involved in the determination of vein versus intervein tissue coincides with the final mitotic wave (*20*, *21*). Consistently, we observed cells with ectopically elevated Dpp signaling levels in the intervein territory of Sara mutant wings but not wild-type wings (Fig. 4, J and K), as well as corresponding morphological defects such as branching or partial duplication (Fig. 4, L to Q).

Why do daughter cells retain the Dpp signaling levels of their mother across mitosis, if they are able to read the extracellular gradient of Dpp again after division? We speculate that our observations might be related to the phenomenon of cellular memory of activin signaling in *Xenopus*, where cells remember activation levels for 3 to 6 hours (even across mitosis) (*22*, *23*) because of the retention of activated receptors within the endocytic pathway (*24*). Dpp signaling in flies does not show long-term memory over several cell generations (*25*). However, Dpp signaling may well exhibit short-term memory of a few hours, which would buffer against signaling fluctuations. Uneven distribution of signaling molecules during mitosis (as in Sara mutants) would then generate a situation in which one of the daughter cells may exhibit signaling levels above the levels corresponding to its actual position. Such discontinuities compromise the robustness of the interpretation of the gradient but will to some extent be compensated by *brinker*-dependent apoptosis (*17*). Our observations thus imply a double mechanism to ensure robustness in the interpretation of the gradient: first, error prevention by preempting the appearance of discontinuities after mitosis through Sara and then, should discontinuities appear, error correction through proofreading and apoptosis (*17*, *18*).

References and Notes

1. M. Gonzalez-Gaitan, *Nat. Rev. Mol. Cell Biol.* **4**, 213 (2003).
2. T. Tsukazaki, T. A. Chiang, A. F. Davison, L. Attisano, J. L. Wrana, *Cell* **95**, 779 (1998).
3. Materials and methods are available as supporting material on *Science* Online.
4. E. Panopoulou *et al.*, *J. Biol. Chem.* **277**, 18046 (2002).
5. C. Raiborg, K. G. Bache, A. Mehlum, E. Stang, H. Stenmark, *EMBO J.* **20**, 5008 (2001).
6. D. J. Katzmann, C. J. Stefan, M. Babst, S. D. Emr, *J. Cell Biol.* **162**, 413 (2003).
7. M. Sachse, S. Urbe, V. Oorschot, G. J. Strous, J. Klumperman, *Mol. Biol. Cell* **13**, 1313 (2002).
8. D. J. Gillooly *et al.*, *EMBO J.* **19**, 4577 (2000).
9. J. Gruenberg, H. Stenmark, *Nat. Rev. Mol. Cell Biol.* **5**, 317 (2004).
10. G. M. Di Guglielmo, C. Le Roy, A. F. Goodfellow, J. L. Wrana, *Nat. Cell Biol.* **5**, 410 (2003).
11. D. Bennett, L. Alphey, *Nat. Genet.* **31**, 419 (2002).
12. R. R. Adams, A. A. Tavares, A. Salzberg, H. J. Bellen, D. M. Glover, *Genes Dev.* **12**, 1483 (1998).
13. G. Emery *et al.*, *Cell* **122**, 763 (2005).
14. B. Riggs *et al.*, *J. Cell Biol.* **163**, 143 (2003).
15. S. Winkler *et al.*, *Genome Res.* **15**, 718 (2005).
16. A. A. Teleman, S. M. Cohen, *Cell* **103**, 971 (2000).
17. E. Moreno, K. Basler, G. Morata, *Nature* **416**, 755 (2002).
18. T. Adachi-Yamada, M. B. O'Connor, *Dev. Biol.* **251**, 74 (2002).
19. A. Perez-Garijo, F. A. Martin, G. Morata, *Development* **131**, 5591 (2004).
20. J. F. de Celis, *Development* **124**, 1007 (1997).
21. M. Milan, S. Campuzano, A. Garcia-Bellido, *Proc. Natl. Acad. Sci. U.S.A.* **93**, 11687 (1996).
22. P. Y. Bourillot, N. Garrett, J. B. Gurdon, *Development* **129**, 2167 (2002).
23. S. Dyson, J. B. Gurdon, *Cell* **93**, 557 (1998).
24. J. Jullien, J. Gurdon, *Genes Dev.* **19**, 2682 (2005).
25. K. Weigmann, S. M. Cohen, *Development* **126**, 3823 (1999).

26. We thank C. P. Heisenberg, M. Zerial, and C. Gonzalez for comments on the manuscript; D. Backasch for excellent technical assistance; M. Wilsch-Braeuninger for help with electron microscopy; S. Winkler for her work on TILLING; and D. Glover, H. Bellen, and H. Steller for the Pavarotti, Hrs, and Hid antisera, respectively. This work was supported by the Max Planck Society, Human Frontier Science Program, Deutsche Forschungsgemeinschaft, and Volkswagen foundation.

Supporting Online Material

www.sciencemag.org/cgi/content/full/314/5802/1135/DC1
Materials and Methods
SOM Text
Figs. S1 to S16
Table S1
References

14 July 2006; accepted 19 September 2006
10.1126/science.1132524

Abortive Initiation and Productive Initiation by RNA Polymerase Involve DNA Scrunching

Andrey Revyakin,[1,2]* Chenyu Liu,[1,2,3] Richard H. Ebright,[1]† Terence R. Strick[2,3]†

Using single-molecule DNA nanomanipulation, we show that abortive initiation involves DNA "scrunching"—in which RNA polymerase (RNAP) remains stationary and unwinds and pulls downstream DNA into itself—and that scrunching requires RNA synthesis and depends on RNA length. We show further that promoter escape involves scrunching, and that scrunching occurs in most or all instances of promoter escape. Our results support the existence of an obligatory stressed intermediate, with approximately one turn of additional DNA unwinding, in escape and are consistent with the proposal that stress in this intermediate provides the driving force to break RNAP-promoter and RNAP-initiation-factor interactions in escape.

Transcription initiation involves a series of reactions (*1*–*3*). RNA polymerase (RNAP) binds to promoter DNA to yield an RNAP-promoter closed complex (RP_c). RNAP then unwinds ~1 turn of DNA surrounding the transcription start site to yield an RNAP-promoter open complex (RP_o). RNAP then enters into abortive cycles of synthesis and release of short RNA products as an RNAP-promoter initial transcribing complex (RP_{itc}) and, upon synthesis of an RNA product ~9 to 11 nucleotides (nt) in length, escapes the promoter and enters into productive synthesis of RNA as an RNAP-DNA elongation complex (RD_e).

The mechanism by which the RNAP active center translocates in abortive initiation and promoter escape has remained unclear. It has remained unclear because of two seemingly contradictory observations. First, RNA products up to ~8 to 10 nt in length are synthesized in

abortive initiation (*4*–*6*); thus, the RNAP active center translocates relative to DNA in abortive initiation. Second, DNA-footprinting results indicate that the upstream boundary of the DNA segment protected by RNAP is the same in RP_o and in RP_{itc} engaged in abortive synthesis (*7*–*10*); thus, RNAP appears not to translocate relative to DNA in abortive initiation. To reconcile the observation that the RNAP active center translocates in abortive initiation with the observation that RNAP appears not to translocate in abortive initiation, three models have been proposed: (i) "scrunching," which invokes contraction of DNA; (ii) "inchworming," which invokes expansion of RNAP; and (iii) "transient excursions," which invokes transient cycles of forward and reverse RNAP translocations with long intervals between cycles (Fig. 1A) (*4*, *7*, *9*–*12*) [see also proposals for structurally unrelated single-subunit RNAP derivatives (*13*–*19*)].

In previous work, we have developed a single-molecule DNA nanomanipulation approach that detects RNAP-dependent DNA unwinding with ~1–base pair (bp) resolution and ~1-s temporal resolution, and we have applied this approach to detect and characterize RNAP-dependent promoter unwinding upon formation of RP_o (Fig. 1B and fig. S1) (*20*–*22*). In this work, we have applied this approach to test the scrunching model for RNAP-active-center translocation in abortive initiation and promoter escape (Fig. 1A) (*4*, *7*, *11*, *12*). The scrunching model—and only the scrunching model—postulates net changes in RNAP-dependent DNA unwinding during abortive initiation and promoter escape (*23*). Specifically, the scrunching model postulates that RNAP pulls downstream DNA into itself; for each base pair that RNAP pulls into itself, a base pair must be broken and must be maintained broken, and, correspondingly, there must be 1 bp of additional DNA unwinding.

Our first set of experiments addressed abortive initiation occurring in complexes engaged in iterative abortive initiation [complexes prepared with the use of subsets of nucleoside triphosphates (NTPs) insufficient to permit promoter escape and productive initiation]. Our primary experimental system was the T5 N25 promoter, a classic model system for analysis of abortive initiation and promoter escape (*11*) (fig. S2). The initial transcribed sequence of the N25 promoter has no C or G residues in the first 8 nt (fig. S2); therefore, upon preparation of RP_o at the N25 promoter and addition of adenosine triphosphate (ATP) and uridine triphosphate (UTP), one obtains RP_{itc} engaged in iterative abortive synthesis of RNA products up to 8 nt in length ($RP_{itc,\leq 8}$; fig. S2). We also analyzed the N25A5C promoter, a derivative of the N25 promoter that has an altered initial transcribed sequence (fig. S3). With the N25A5C promoter, with appropriate NTP subsets, one obtains RP_{itc} engaged in iterative abortive synthesis of products up to 4 nt in length ($RP_{itc,\leq 4}$) and 8 nt in length ($RP_{itc,\leq 8}$) (fig. S3).

To determine whether scrunching occurs in abortive initiation, we quantified RNAP-dependent DNA unwinding at the N25 promoter in RP_o (0 NTPs) and in $RP_{itc,\leq 8}$ (ATP + UTP) (Fig. 2, A and D). Comparison of the amplitudes of transitions in RP_o and in $RP_{itc,\leq 8}$ in representative single-molecule time traces indicates that the amplitude of transitions is greater in $RP_{itc,\leq 8}$ (Fig. 2A, left). Comparison of the histograms shows clearly that the amplitude of transitions is greater in $RP_{itc,\leq 8}$ (Fig. 2A, right). By combining data obtained with positively supercoiled DNA and data obtained with negatively supercoiled DNA, we can establish unequivocally that there is a difference in DNA unwinding in RP_o and $RP_{itc,\leq 8}$, and we can extract the extent of that difference; namely, upon transition from RP_o to $RP_{itc,\leq 8}$, there is an increase in unwinding of 5 ± 1 bp (Fig. 2D). Consistent with these results, we find that, upon transition from RP_o to $RP_{itc,\leq 8}$ at the N25 promoter, the downstream boundary of the potassium-permanganate-sensitive promoter region shifts from position +2 to position +8, implying an increase in DNA unwinding of 6 bp (fig. S4). We conclude that scrunching occurs in abortive initiation.

[1]Howard Hughes Medical Institute, Waksman Institute, and Department of Chemistry, Rutgers University, Piscataway, NJ 08854, USA. [2]Cold Spring Harbor Laboratory, Cold Spring Harbor, NY 11724, USA. [3]Institut Jacques Monod, Centre National de la Recherche Scientifique UMR 7592 and Universités de Paris VI et Paris VII, 2 Place Jussieu, 75251 Paris Cedex 05, France.

*Present address: Howard Hughes Medical Institute and Department of Molecular and Cell Biology, 16 Barker Hall, University of California, Berkeley, CA 94720–3204, USA.
†To whom correspondence should be addressed. E-mail: strick@ijm.jussieu.fr (T.R.S.); ebright@waksman.rutgers.edu (R.H.E.)

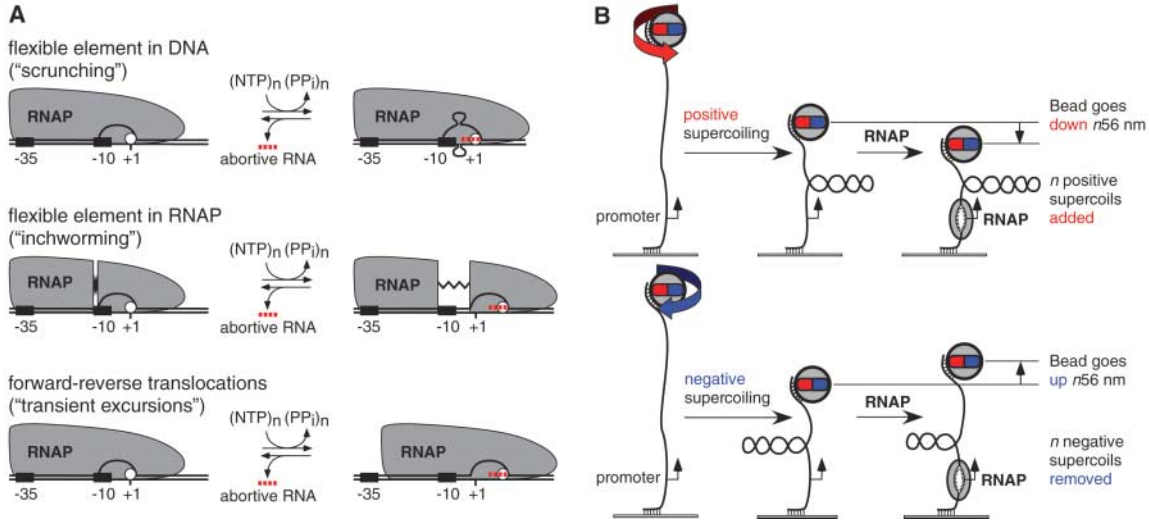

Fig. 1. Background and experimental approach. (**A**) Models for RNAP–active-center translocation in abortive initiation. (Top) The "scrunching" model invokes a flexible element in DNA [(*4*, *7*, *11*, *12*); see also (*13*–*19*)]. In each cycle of abortive initiation, RNAP unwinds downstream DNA and pulls it into itself, accommodating the accumulated DNA as single-stranded bulges in the unwound region; upon release of the abortive RNA, RNAP extrudes the internalized DNA. (Middle) The "inchworming" model invokes a flexible element in RNAP (*9*, *10*). In each cycle of abortive initiation, a module of RNAP containing the active center (white circle) detaches from the remainder of RNAP and translocates downstream; upon release of the abortive RNA, this module of RNAP reverse translocates. (Bottom) The "transient-excursions" model invokes abortive cycles that are transient–too short in lifetime and too infrequent in occurrence to be detected in a time-averaged, population-averaged approach, such as DNA footprinting (*7*). In each cycle of abortive initiation, RNAP translocates downstream as a unit; upon release of the abortive RNA, RNAP reverse translocates as a unit. (**B**) Experimental approach (fig. S1) (*20*–*22*). The end-to-end extension of a mechanically stretched, negatively supercoiled (top) or positively supercoiled (bottom), single DNA molecule containing a single promoter is monitored. Unwinding of *n* turns of DNA by RNAP results in the compensatory loss of *n* negative supercoils or gain of *n* positive supercoils, and a readily detectable, nanometer-scale (*n* times 56 nm), movement of the bead.

To determine whether scrunching requires RNA synthesis, we performed a control experiment in which we provided only the initiating nucleotide, ATP ($RP_{itc,\leq 1}$) (Fig. 2, B and D, and figs. S2 and S5). We also performed a control experiment in which we provided ATP, UTP, and rifampicin, an inhibitor that blocks synthesis of RNA products >2 nt in length ($RP_{itc,\leq 2}$) (Fig. 2, C and D, and figs. S2 and S5). In both experiments, scrunching was not observed (Fig. 2, B and D and C and D). We conclude that scrunching requires RNA synthesis and, more particularly, that scrunching requires synthesis of an RNA product >2 nt in length.

To determine whether the extent of scrunching correlates with RNA length, we quantified RNAP-dependent DNA unwinding at the N25A5C promoter in RP_o (no NTPs), $RP_{itc,\leq 4}$ (ATP + UTP), and $RP_{itc,\leq 8}$ [ATP + UTP+ cytidine triphosphate (CTP)] (Fig. 3, A and B, and figs. S3 and S6). We observed successive, stepwise increases in the amplitudes of transitions (Fig. 3A) and in the corresponding extents of DNA unwinding (Fig. 3B). We observed increases in DNA unwinding of 2 ± 1 bp upon transition from RP_o to $RP_{itc,\leq 4}$ (Fig. 3B) and 5 ± 1 bp upon transition from RP_o to $RP_{itc,\leq 8}$ (Fig. 3B). Within experimental error, the observed increases in unwinding in the preceding experiments and in this experiment agree with the quantitative predictions of the simplest version of the scrunching model, in which increases in unwinding are predicted to equal $N - 2$, where N is the length of the RNA in nucleotides (Fig. 3C). [In the simplest version of the scrunching model, the RNAP active center is predicted to be able to make an RNA product 2 nt in length without translocation, but to need to translocate, and to scrunch, to make longer RNA products; thus, the increase in unwinding is predicted to equal $N - 2$ (Fig. 3C).] We conclude that the extent of scrunching in abortive initiation correlates with RNA length and that it correlates quantitatively as predicted by the simplest model of scrunching.

In each of the preceding experiments, complexes engaged in abortive synthesis and release of RNA products >2 nt in length were observed to be present predominantly in the scrunched state; cycles of transitions between the scrunched state and the unscrunched state having the extent of unwinding in RP_o were not observed (Fig. 2A and figs. S5 and S6). We infer that, at the promoters and saturating NTP concentrations studied, abortive-product synthesis and scrunching are fast relative to abortive-product release and unscrunching, and also are fast relative to the second-scale temporal resolution of our method. Consistent with this inference, recently published results indicate that, at a consensus promoter, at saturating NTP concentrations, the rate-limiting step in abortive initiation is abortive-product release and RNAP-active-center reverse translocation (*24*).

Our results for abortive initiation receive unequivocal support from the companion paper (*25*), which analyzes abortive initiation by means of an independent single-molecule method: single-molecule fluorescence resonance energy transfer (in which scrunching is detected as a decrease in distance between the DNA segments upstream and downstream of the unwound region).

Our second set of experiments addressed promoter escape in complexes engaged in productive initiation (complexes prepared in the presence of all four NTPs). For these experiments, we used DNA constructs having the N25 promoter, followed by a 400- or 100-bp–transcribed region, followed by a terminator (N25-400-tR2 and N25-100-tR2) (fig. S7). These constructs allowed us to monitor complete transcription cycles in the presence of all four NTPs, monitoring promoter unwinding, promoter escape, elongation, and termination, in real time. In addition, as a result of the presence of a terminator, these constructs automatically recycled the DNA molecule, facilitating the collection of large data sets ($n > 100$). (After each transcription cycle, RNAP dissociated from the DNA molecule, rendering the DNA molecule available for the next transcription cycle.) For these experiments, we also used shorter (2 versus 4 kb) DNA molecules (fig. S8) (*22*). This resulted in a decrease in noise and an increase in spatial and temporal resolution.

To determine whether scrunching occurs in productive initiation, we collected and analyzed single-molecule time traces in experiments with

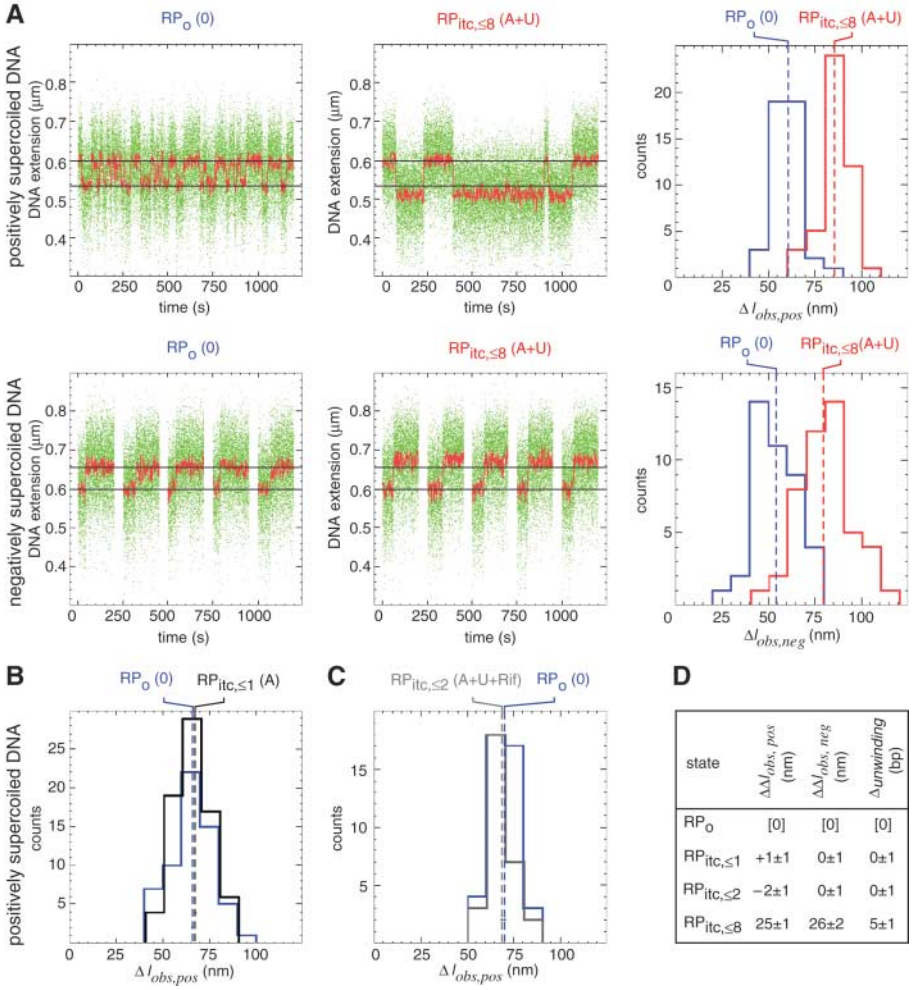

Fig. 2. Scrunching occurs in abortive initiation. (**A**) Single-molecule time traces and transition-amplitude histograms for RP_o (0 NTPs) and $RP_{itc,\leq 8}$ (ATP+UTP) at the N25 promoter. Data for positively and negatively supercoiled DNA are at the top and bottom, respectively. Green points, raw data (30 frames per s); red points, averaged data (1-s window); dashed lines in histograms, means; $\Delta l_{obs,pos}$, transition amplitude with positively supercoiled DNA; $\Delta l_{obs,neg}$, transition amplitude with negatively supercoiled DNA. (**B**) Transition-amplitude histogram for $RP_{itc,\leq 1}$ (from control experiment providing only ATP). (**C**) Transition-amplitude histogram for $RP_{itc,\leq 2}$ (from control experiment providing ATP, UTP, and rifampicin). (**D**) Differences in $\Delta l_{obs,pos}$, $\Delta l_{obs,neg}$, and unwinding relative to values in RP_o (mean ± SE).

N25-400-tR2 and N25-100-tR2 in the presence of all four NTPs (Fig. 4 and fig. S9). Representative single-molecule time traces exhibited series of events, in which each individual event corresponded to a complete transcription cycle, from promoter unwinding through termination (Fig. 4A and fig. S9; events underscored in black). The events were markedly uniform in duration and overall form (Fig. 4A and fig. S9). (Struck by this uniformity, we refer to these time traces as "EKG strips of transcription.") We parsed each event into four unwinding and rewinding transitions: a first transition from the initial state to a state having the extent of unwinding in RP_o; a second transition to a state having the extent of unwinding in the scrunched RP_{itc}; a third transition to a state having an extent of unwinding comparable but not identical to that in RP_o; and a fourth transition returning to the initial state (Fig. 4A and figs. S9 and S10). We assigned these four transitions to the formation of RP_o, the formation of RP_{itc} (with scrunching), the formation of RD_e (with reversal of scrunching), and termination. Scrunching occurred in these events (Fig. 4, A and B, and figs. S9 and S10). Scrunching was manifested as the "overshoot" in unwinding that followed formation of RP_o and preceded formation of RD_e. The observed extent of scrunching was 9 ± 2 bp (Fig. 4B), which agreed, to the base pair, with the predicted extent of scrunching under the $N - 2$ rule (Fig. 3C). [Promoter escape at N25 occurs upon synthesis of an RNA product having a length, N, of 11 nt (fig. S2B).] We conclude that scrunching occurs in promoter escape in productive initiation.

Extensive control experiments documented the assignment of transitions in the preceding paragraph (figs. S11 to S14). When experiments were performed in the absence of NTPs, yielding RP_o, only transition 1 was observed (fig. S11A). When experiments were performed with an NTP subset yielding $RP_{itc,\leq 8}$, only transitions 1 and 2 were observed (fig. S11B). When experiments were performed with an NTP subset yielding a halted elongation complex, $RD_{e,29}$, only transitions 1, 2, and 3 were observed (fig. S11C). When the remaining NTPs were added back to any of the preceding cases, the full process was recapitulated, with full cycles of transcription (fig. S11, A to C). When the terminator was omitted, only transitions 1, 2, and 3 were observed (fig. S12). When the length of the transcribed region was varied, the duration of the phase between transitions 3 and 4 changed, and it changed according to a relationship suggesting an elongation rate of ~10 nt/s [which equals the expected elongation rate for the NTP concentration and temperature (*26*–*29*)] (figs. S13 and S14). Again, we conclude that scrunching occurs in promoter escape in productive initiation.

To determine whether scrunching occurs in few, many, or all, productive initiation events, we compared the number of transcription cycles that exhibited detectable scrunches to the number of transcription cycles that did not (Fig. 4C). Fully 80% of transcription cycles exhibited a detectable scrunch (Fig. 4C). Thus, most transcription cycles involve scrunching. This percentage, however, represents an underestimate, because the temporal resolution of our approach is insufficient to detect "fast" scrunches (scrunches that have a duration <1 s). From the observed distribution of scrunch lifetimes, we estimate that 20% of scrunches have a duration <1 s (Fig. 4D). Based on the percentage of transcription cycles that exhibit a detectable scrunch (80%) and the estimated percentage of scrunches that are not detected because they have a duration <1 s (20%), it is apparent that ~100% of transcription cycles involve scrunching. We conclude that scrunching occurs in all, or nearly all, transcription cycles. We further conclude that scrunching may be obligatory for promoter escape in productive initiation.

Our overall conclusions are as follows: abortive initiation involves scrunching. Promoter escape involves scrunching. Promoter escape may, and we propose does, involve obligatory scrunching. Promoter escape may, and we propose does, involve an obligatory "stressed

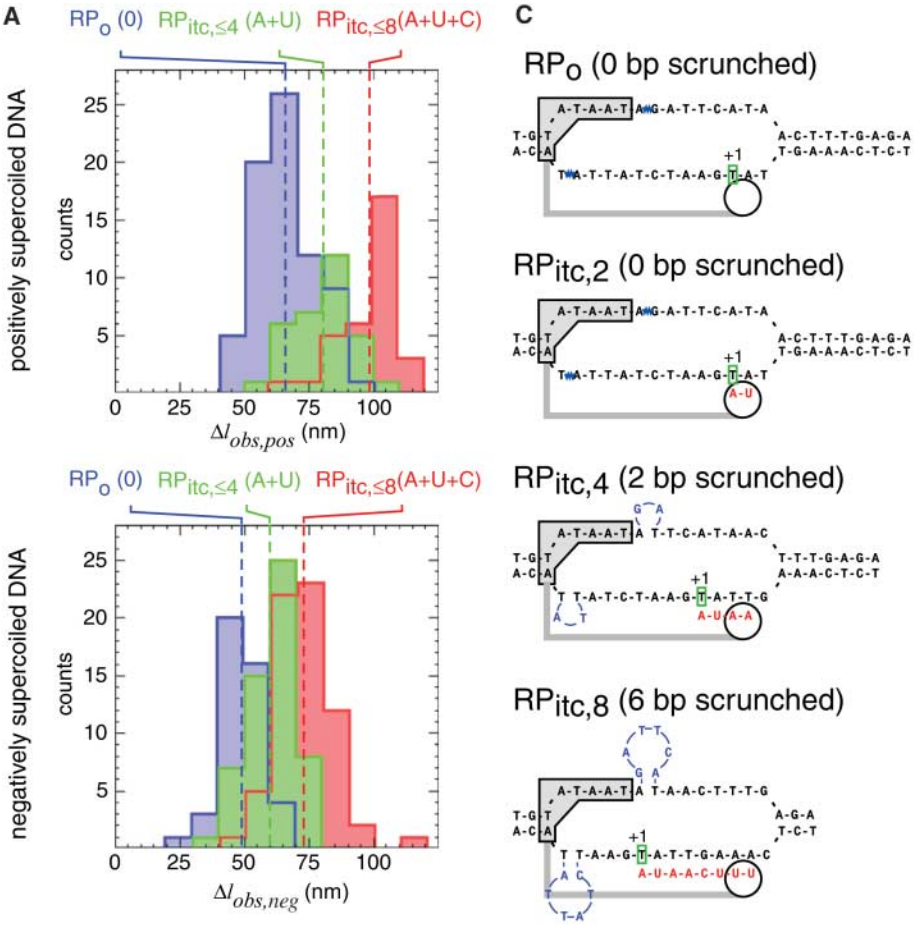

B

state	$\Delta\Delta l_{obs,pos}$ (nm)	$\Delta\Delta l_{obs,neg}$ (nm)	$\Delta_{unwinding}$ (bp)
RP_o	[0]	[0]	[0]
$RP_{itc,\leq 4}$	15±1	10±2	2±1
$RP_{itc,\leq 8}$	33±1	23±2	5±1

Fig. 3. The extent of scrunching correlates with the length of the RNA product. (**A**) Transition-amplitude histograms for RP_o (0 NTPs), $RP_{itc,\leq 4}$ (ATP+UTP), and $RP_{itc,\leq 8}$ (ATP+UTP+CTP) at the N25A5C promoter. Data for positively and negatively supercoiled DNA are at the top and bottom, respectively. (**B**) Differences in $\Delta l_{obs,pos}$, $\Delta l_{obs,neg}$, and unwinding relative to values in RP_o (mean ± SE). (**C**) Prediction of scrunching model: number of base pairs scrunched equals $N - 2$, where N is the length of the RNA product. Sequence-specific RNAP-promoter interactions that define the upstream boundary of the unwound region are indicated by a gray box; RNAP structural elements that constrain the spacing between the upstream boundary of the unwound region and the RNAP active center are indicated by a gray bar; the RNAP active center is indicated by a white circle; the RNA product is in red; position +1 of the template DNA strand is in green; scrunched DNA nucleotides are in blue [(and are positioned as proposed in (*25*)].

intermediate," as originally suggested two decades ago [(*9*); see also (*11*)].

At a typical promoter, promoter escape occurs only after synthesis of an RNA product ~9 to 11 nt in length (*1*–*11*) and thus can be inferred to require scrunching of ~7 to 9 bp ($N-2$, where N = ~9 to 11; Fig. 3C). Assuming an energetic cost of base-pair breakage of ~2 kcal/mol per bp (*30*), it can be inferred that, at a typical promoter, a total of ~14 to 18 kcal/mol of base-pair–breakage energy is accumulated in the stressed intermediate. This free energy is high relative to the free energies for RNAP-promoter interaction [~7 to 9 kcal/mol for sequence-specific component of RNAP-promoter interaction (*1*)] and RNAP-initiation-factor interaction [~13 kcal/mol for transcription initiation factor σ^{70} (*31*)]. We propose that our results demonstrate the existence of an obligatory stressed intermediate, and we propose that the energy accumulated in that obligatory stressed intermediate is the energy that drives the disruption of interactions between RNAP and promoter DNA and between RNAP and initiation factors and, thus, is the energy that drives the transition from initiation to elongation.

References and Notes

1. M. T. Record Jr., W. Reznikoff, M. Craig, K. McQuade, P. Schlax, in Escherichia coli *and* Salmonella*: Cellular and Molecular Biology*, F. C. Neidhardt *et al.*, Eds. (American Society for Microbiology, Washington, DC, 1996), vol. 1, pp. 792–820.
2. B. A. Young, T. M. Gruber, C. A. Gross, *Cell* **109**, 417 (2002).
3. K. Murakami, S. Darst, *Curr. Opin. Struct. Biol.* **13**, 31 (2003).
4. A. J. Carpousis, J. D. Gralla, *Biochemistry* **19**, 3245 (1980).
5. M. A. Grachev, E. F. Zaychikov, *FEBS Lett.* **115**, 23 (1980).
6. L. Munson, W. Reznikoff, *Biochemistry* **20**, 2081 (1981).
7. A. J. Carpousis, J. D. Gralla, *J. Mol. Biol.* **183**, 165 (1985).
8. A. Spassky, *J. Mol. Biol.* **188**, 99 (1986).
9. D. C. Straney, D. M. Crothers, *J. Mol. Biol.* **193**, 267 (1987).
10. B. Krummel, M. Chamberlin, *Biochemistry* **28**, 7829 (1989).
11. L. M. Hsu, *Biochim. Biophys. Acta* **1577**, 191 (2002).
12. M. Pal, A. S. Ponticelli, D. S. Luse, *Mol. Cell* **19**, 101 (2005).
13. G. M. Cheetham, D. Jeruzalmi, T. A. Steitz, *Nature* **399**, 80 (1999).
14. G. M. Cheetham, T. A. Steitz, *Science* **286**, 2305 (1999).
15. L. G. Brieba, R. Sousa, *EMBO J.* **20**, 6826 (2001).
16. M. Jiang, M. Rong, C. Martin, W. T. McAllister, *J. Mol. Biol.* **310**, 509 (2001).
17. C. Liu, C. T. Martin, *J. Biol. Chem.* **277**, 2725 (2002).
18. E. A. Esposito, C. T. Martin, *J. Biol. Chem.* **279**, 44270 (2004).
19. P. Gong, E. A. Esposito, C. T. Martin, *J. Biol. Chem.* **279**, 44277 (2004).
20. A. Revyakin, J.-F. Allemand, V. Croquette, R. H. Ebright, T. R. Strick, *Methods Enzymol.* **370**, 577 (2003).
21. A. Revyakin, R. H. Ebright, T. R. Strick, *Proc. Natl. Acad. Sci. U.S.A.* **101**, 4776 (2004).
22. A. Revyakin, R. H. Ebright, T. R. Strick, *Nat. Methods* **2**, 127 (2005).
23. The scrunching model postulates that, during abortive initiation, unwinding of downstream DNA base pairs occurs and rewinding of upstream DNA base pairs does not occur, and thus that there is a net increase in DNA unwinding (see length of unwound region in Fig. 1A). In contrast, the inchworming and transient-excursions models postulate that both unwinding of downstream DNA base pairs and rewinding of upstream DNA base pairs occur and thus that there is no net change in DNA unwinding (see length of unwound regions in Fig. 1, B and C).
24. E. Margeat *et al.*, *Biophys. J.* **90**, 1419 (2006).
25. A. Kapanidis *et al.*, *Science* **314**, 1144 (2006).
26. M. D. Wang *et al.*, *Science* **282**, 902 (1998).
27. K. Adelman *et al.*, *Proc. Natl. Acad. Sci. U.S.A.* **99**, 13538 (2002).
28. E. A. Abbondanzieri, W. J. Greenleaf, J. W. Shaevitz, R. Landick, S. M. Block, *Nature* **438**, 460 (2005).
29. E. A. Abbondanzieri, J. W. Shaevitz, S. M. Block, *Biophys. J.* **89**, L61 (2005).
30. K. J. Breslauer, R. Frank, H. Blocker, L. A. Marky, *Proc. Natl. Acad. Sci. U.S.A.* **83**, 3746 (1986).
31. S. C. Gill, S. E. Weitzel, P. H. von Hippel, *J. Mol. Biol.* **220**, 307 (1991).

32. We thank S. Borukhov, L. Hsu, and E. Nudler for plasmids and for discussion. This work was supported by Cold Spring Harbor Laboratory, Centre National de la Recherche Scientifique Action Thematique Incitative et sur Programme, Fondation pour la Recherche Médicale, Fondation Fourmentin-Guilbert, European Molecular Biology Organization Young Investigator Programme, and City of Paris grants (to T.R.S.), and by NIH grant GM41376 and a Howard Hughes Medical Investigatorship (to R.H.E.).

Supporting Online Material

www.sciencemag.org/cgi/content/full/314/5802/1139/DC1
Materials and Methods
Figs. S1 to S15
References

16 June 2006; accepted 29 September 2006
10.1126/science.1131398

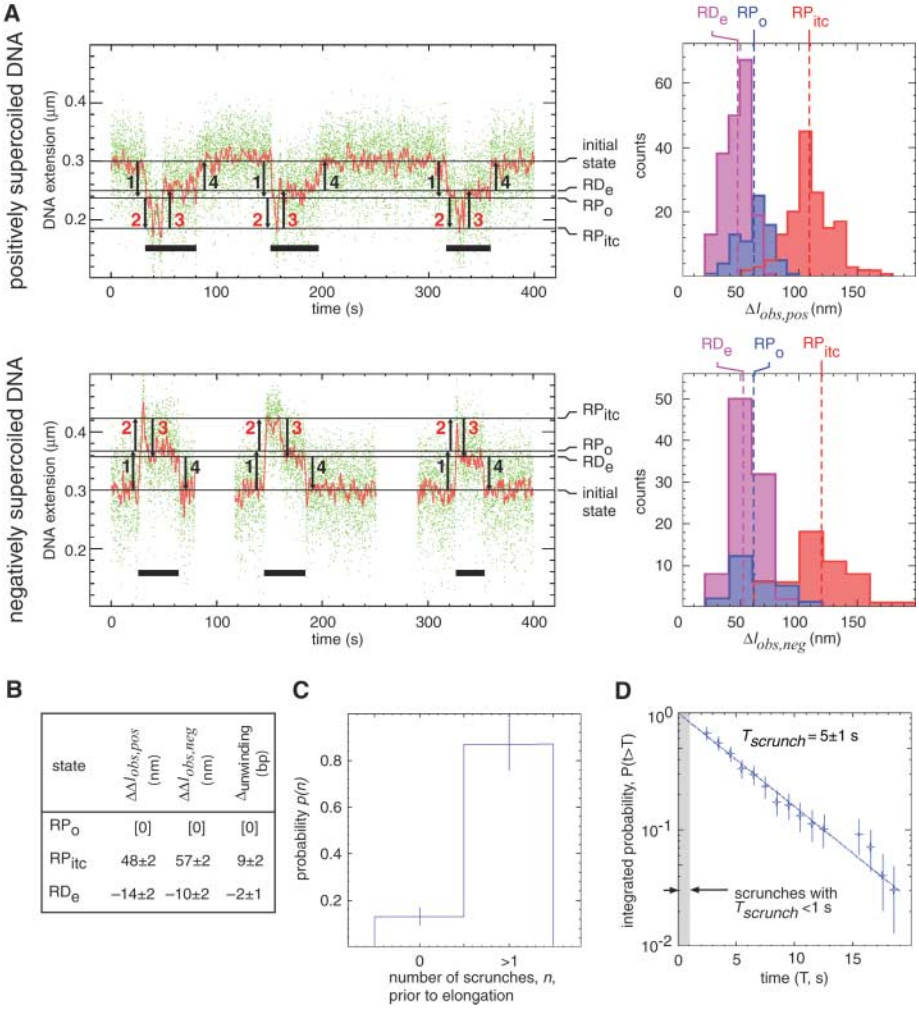

Fig. 4. Scrunching occurs in promoter escape in productive initiation. (**A**) Single-molecule time traces and transition-amplitude histograms for complete transcription cycles on N25-400-tR2 in the presence of all four NTPs. Data for positively and negatively supercoiled DNA are at the top and bottom, respectively. Transcription cycles are indicated by horizontal black bars; unwinding and rewinding transitions are indicated by numbered arrows (red numbered arrows for scrunching and reversal of scrunching); and states are indicated by horizontal lines and labeled on the right. (**B**) Differences in $\Delta l_{obs,pos}$, $\Delta l_{obs,neg}$, and unwinding relative to values in RP_o. (**C**) Fraction of transcription cycles exhibiting at least one detectable scrunch (mean ± SEM; $n = 100$). (**D**) Distribution of scrunch lifetime [measured from midpoint of transition 2 to midpoint of transition 3 ($n = 100$)]. Error bars indicate statistical error.